Available online at www.sciencedirect.com
ScienceDirect
Journal of Power Sources 161 (2006) 806–812
JOURNAL OF POWER SOURCES
www.elsevier.com/locate/jpowsour

Silver-cobalt bimetallic particles for oxygen reduction in alkaline media

F.H.B. Lima, J.F.R. de Castro, Edson A. Ticianelli *

Instituto de Química de São Carlos, USP, CP 780, 13560-970 São Carlos, SP, Brazil

Received 24 April 2006; received in revised form 2 June 2006; accepted 6 June 2006
Available online 25 July 2006

Abstract

The kinetics of the oxygen reduction reaction (ORR) was studied on ultra thin layer electrodes formed by bimetallic Ag-Co nanoparticles dispersed on a carbon powder (Ag-Co/C) in KOH electrolyte. The morphological features of the materials were studied by transmission electron microscopy (TEM) and X-ray diffraction (XRD). Cyclic voltammetry and steady state polarization measurements for the ORR were obtained using the rotating ring/disk electrode (RRDE) technique. TEM measurements for the bimetallic Ag-Co/C catalysts showed a heterogeneous crystallite size distribution and, together with XRD, suggested the presence of a segregated phase of cobalt, mainly as Co_3O_4. The characterization of the materials by XRD also showed a negligible decrease in the Ag face centered cubic (fcc) lattice parameter, which was ascribed to a negligible Co insertion into the Ag structure. Levich plots obtained from rotating disk electrode data have shown a higher number of electrons for the Ag-Co/C materials, compared to Ag/C. The polarization results showed higher activity for the ORR on Ag-Co/C materials in comparison to Ag/C.

Keywords: Silver; Bimetallic particles; Electrocatalysis; Oxygen reduction; Fuel cells

1. Introduction

Several studies have been done aiming to increase the platinum electrocatalytic performance for the oxygen reduction reaction (ORR) [1–10]. Some authors have reported that on several Pt alloys, such as Pt–V, Pt–Co, Pt–Cr, Pt–Fe, etc., there is an increase in the kinetics of the ORR electrocatalysis compared to pure Pt, and this fact has been attributed to changes in the Pt–Pt bond distance, number of Pt nearest neighbors, electron density of states in the Pt 5d band, and nature and coverage of surface oxide layers [2,4–8]. In recent work, Nørskov and co-workers [11–14] have shown that the catalytic activity of different metals can be rationalized in terms of the energy of the d-band center. The study has also explained the activity enhancement for the ORR of some alloys, such as Pt–Co, based on the lowering of the Pt–O^- bond strength. The presence of the Co atoms in the Pt lattice structure modifies the electronic and chemical properties of the Pt atoms leading to a down shift of the Pt d-band center, which lowers the Pt reactivity and, as a consequence, decreases the Pt-oxide surface coverage.

Despite the extensive research carried out aiming at performance improvement and/or lowering the Pt mass content in the electrocatalysts, the cost associated to this material is still a drawback for full commercial application of fuel cells. Some studies have been done trying to search for an abundant, inexpensive, stable and efficient electrocatalytic material as a substitute for Pt-based oxygen cathodes [15–17]. In this context, carbon-supported silver particles (Ag/C) are a good candidate for application as the catalyst for oxygen cathodes in alkaline solutions [18–20], such as alkaline fuel cells and metal/air batteries, this is because its relatively high activity for the O_2 reduction and the occurrence of an ORR mechanism via 4-electrons.

Silver binds oxygen considerably less strongly than Pt. So, if the d-band center position of Pt is close to the optimum [10], then this would suggest that pure Ag is less active for O_2 reduction than Pt just because the weaker Ag–O_2 interaction makes the breaking of the O–O bond in this catalyst more difficult. In this way, the Ag reactivity or Ag d-band center should be increased for producing stronger Ag–O interactions, leading to easier O–O bond breaking and, consequently, enhancing the ORR kinetics.

In a previous work [21], the ORR was investigated on dispersed Ag–Pt/C alloys having the particles covered by a thin Ag-rich surface layer, so that the participation of the Pt atoms in the electrocatalysis of the ORR is negligible. It was observed

* Corresponding author.
E-mail address: edsont@iqsc.usp.br (E.A. Ticianelli).

0378-7753/$ – see front matter © 2006 Elsevier B.V. All rights reserved.
doi:10.1016/j.jpowsour.2006.06.029

that the activity of the silver atoms in the Ag-rich surface layer of the bimetallic Ag–Pt/C particles is considerably higher than that of the silver atoms in Ag/C. This increased activity was considered a consequence of a high interaction of adsorbed oxygen with Ag on the Ag–Pt/C particles, facilitating the rupture of the O–O bond and increasing the ORR kinetics.

Bard and co-workers [22] have designed several binary and ternary electrocatalysts for the ORR in acid media, consisting of combinations of M–Co, with M = Pd, Au and Ag. The electrocatalytic activity of these materials was examined using the scanning electrochemical microscopy technique. The results have shown that the addition of Co to Pd, Au and Ag clearly decreased the ORR overpotentials. The combinations that exhibited enhanced electrocatalytic activity were then examined as carbon-supported metal particles on a rotating disk electrode. The polarization curves showed excellent agreement with the results on smooth electrodes, with Pd-Co/C and Ag-Co/C exhibiting higher activities when at an atomic ratio of 80:20 of M:Co. The authors have explained the catalytic enhancement assuming a simple mechanism, through which one metal breaks the O–O bond of molecular O_2, and then the adsorbed atomic oxygen atoms migrates to the other metal, where the electroreduction step takes place.

In this work, the oxygen reduction reaction was studied on bimetallic Ag and Co particles dispersed on carbon, in alkaline media. Ag/C and Ag-Co/C (atomic ratios of 3:1 and 1:3 Pt:Co) were synthesized based on chemical reduction of the precursor metal salts, using sodium borohydride. The physical characterization of the materials was carried out using transmission electron microscopy (TEM) and X-ray diffraction (XRD). The electrochemical characteristics were obtained by cyclic voltammetry and steady state polarization curves. The catalytic activity for the ORR was analyzed considering the changes of the Ag properties introduced by Co.

2. Experimental

The electrocatalysts were Ag and Ag-Co dispersed on carbon (Ag/C or Ag-Co/C), 20 wt.% metal/C. The bimetallic particles were home-made with different nominal atomic ratios, ranging from pure Ag, Ag:Co 3:1, Ag:Co 1:3 to pure Co/C. These were prepared by simultaneous reduction of the precursor metal salts $Ag(NO_3)_2$ and $Co(NO_3)_2{\cdot}2H_2O$ (Merck). The reduction process was carried out at 60 °C by drop wise addition of the precursor solution onto a high surface area carbon powder (Vulcan XC-72R) slurry, which was prepared by suspending carbon powder in ultra pure water (Millipore) and ultrasonically blending for 10 min. This is followed by drop wise addition of an excess of a sodium borohydride ($NaBH_4$) solution, for reduction a precipitation of the precursor metal particles. The resulting precipitates were filtered and dried at 60 °C.

The composition of the catalysts was confirmed by energy dispersive X-ray analysis (EDX—LEO model 440). Transmission electron microscopy analyses were carried out using a Philips CM120 microscope. Particle size and phase characterizations were carried out by TEM with dark field observations and selected area electron diffraction pattern (SAEDP). X-ray diffraction (XRD—RIGAKU model RU200B) measurements were carried out in the 2θ range from 10° up to 100° and using Cu Kα radiation (with a scan rate of $2^\circ\ min^{-1}$) for physical properties determination such as lattice structure and crystallite size. The average crystallite size of the Ag particles was estimated using the Ag (1 1 1) peak of the Ag diffraction pattern using the Sherrer equation [23].

The working electrodes were metal/C catalysts deposited as an ultra thin layer over a pyrolitic graphite disk, 5 mm diameter (0.196 cm^2), of a rotating ring/disk electrode (RRDE). The ultra thin layers were prepared starting from an aqueous suspension of 2.0 mg mL^{-1} of the metal/C produced by ultrasonically dispersing in pure water (Millipore) [24]. A 20 μL aliquot of the dispersed suspension was pipetted on the top of the pyrolitic graphite substrate surface. After the evaporation of water, in a low vacuum condition at room temperature, 20 μL of a diluted Nafion solution (5%, Aldrich) were pipetted on the graphite disk surface in order to attach the catalytic particles on the RRDE electrode substrate, and after that, dried under low vacuum. Right after preparation, the electrodes were immersed into de-aerated 1.0 mol L^{-1} KOH electrolyte.

A large area platinum screen served as counter electrode and an Hg/HgO (KOH 1.0 mol L^{-1} KOH) system was used as the reference electrode. All the experiments were carried out in 1.0 mol L^{-1} KOH electrolyte, prepared from high purity reagents (Merck) and water purified in a Milli-Q (Millipore) system. Owing to slight contamination from the Nafion solution, the electrode potentials were cycled several times between −0.88 and 0.55 V versus Hg/HgO in order to produce a clean catalyst surface. To evaluate the ORR kinetic parameters, steady state polarization measurements for the oxygen reduction were carried out in a rotating ring/disk electrode in saturated oxygen conditions by stair step polarization technique, point-by-point using a step of 20 mV and 30 s $step^{-1}$, at several rotation rates. In this system, the ring electrode (gold) was employed to sensor the HO_2^- produced in the working disk electrode. This was made measuring the magnitude of the HO_2^- oxidation current at a constant potential of 0.1 V versus Hg/HgO, where the oxygen reduction currents are negligible. All experiments were conducted at room temperature (25 ± 1 °C), using an AUTOLAB (PGSTAT30) potentiostat.

3. Results and discussion

3.1. Physical properties of the Ag-Co/C bimetallic particles

Figs. 1 and 2 show the bright field TEM images of Ag/C and Co/C samples, respectively. Fig. 1 shows Ag/C particles with rounded shape contrast, with crystallite size distribution in the range of 30–200 nm. Fig. 2 shows Co/C particles with rounded and elongated shapes and particle size distribution in the order of 50 nm. The SAEDP of this area indicates the presence of a cubic phase of Co_3O_4 [25]. The TEM (a) bright and (b) dark field images of the Ag-Co/C 1:3 sample with its corresponding (c) SAEDP are shown in Fig. 3. The dark field image shows two different types of nanostructured morphologies: first, particles with elongated shape and particles sizes close to 8 nm; second,

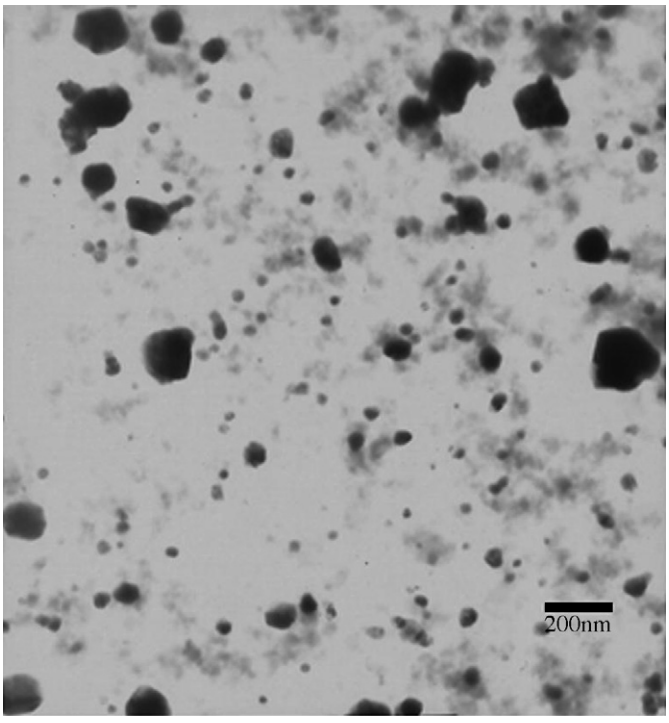

Fig. 1. Bright field TEM images of the Ag supported on Vulcan carbon XC-72 catalyst, deposited on an on amorphous carbon film.

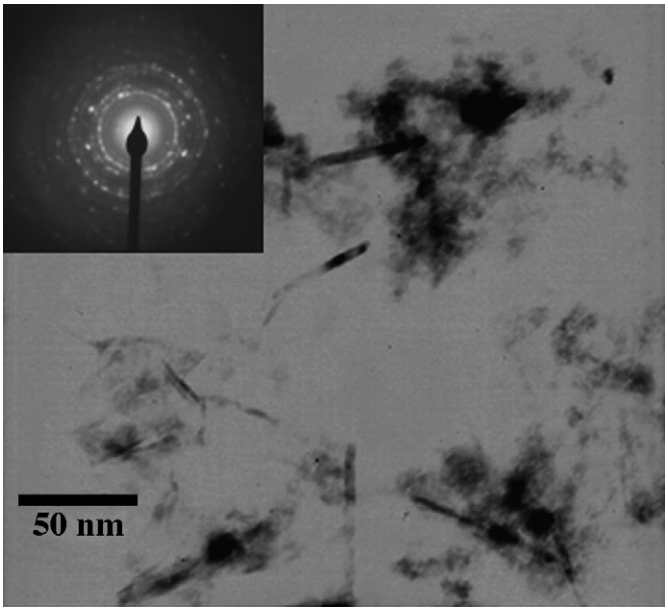

Fig. 2. Bright field TEM images of the Co supported on Vulcan carbon XC-72 catalyst, deposited on an on amorphous carbon film. Inset: selected area electron diffraction pattern (SAEDP).

particles with rounded shape and sizes in the range of 30–70 nm. The SAEDP of these areas indicates the presence of a cubic of Co_3O_4 phase. It is important to mention that the larger particles in the dark field TEM images do not diffract the X-ray, probably because they are agglomerated of catalyst particles covered by a thin layer of carbon or they are just agglomerates of carbon particles. It is important to mention that, in all samples, the particles were homogeneously dispersed throughout the carbon substrate, as observed by imaging other regions of the samples.

Fig. 4 presents the XRD patterns for the different synthesized silver-cobalt materials. The XRD patterns indicate that all silver-cobalt electrocatalysts present the face centered cubic (fcc) structure of silver [25]. There is no shift in the reflection angles, with respect to Ag/C, indicating a negligible cobalt insertion on the Ag lattice. The results also indicate a phase segregation of cobalt mainly as Co_3O_4 and, into lower extent, of Co_2O_3 for the bimetallic Ag-Co/C catalysts. The peak shoulder at ca. 36°, observed for all samples, is due to the presence of boron oxide, which comes from the reducing agent $NaBH_4$ [25]. XRD results were analyzed using the Scherrer equation. The mean crystallite sizes estimated for the Ag/C, Ag-Co/C 3:1 and Ag-Co/C 1:3 catalysts resulted in 24.1, 20.7 and 18.2 nm, respectively.

3.2. Electrochemical characteristics

Fig. 5 shows the cyclic voltammogram (CV) profiles for the silver-cobalt materials, compared to those obtained for Ag/C, Co/C and bulk Ag (inset). As can be seen, the oxide region is very prominent for the silver materials, with the CV clearly presenting only the Ag features [26–30]. The anodic peaks located in the range of 0.2–0.4 V are related to the formation of Ag_2O layers, and the cathodic peak at around 0.15 V is assigned to

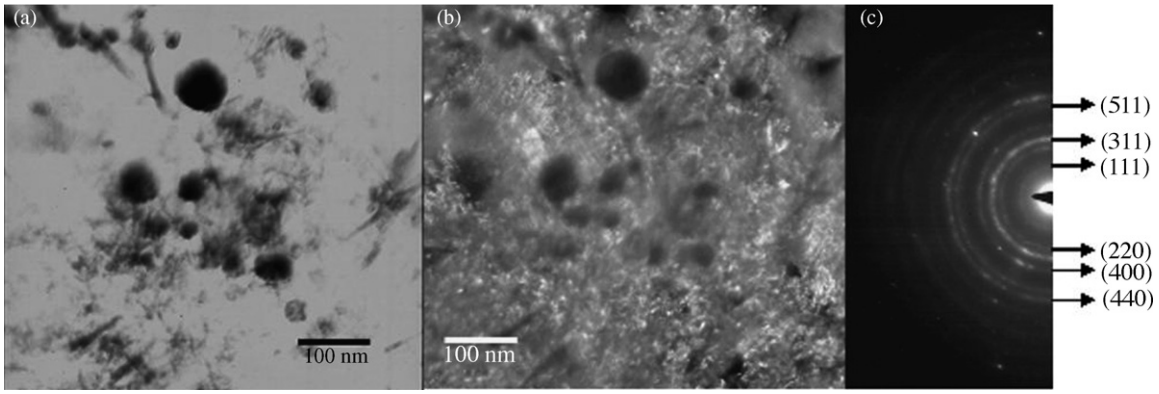

Fig. 3. (a) Bright field, (b) dark field TEM images and (c) selected area electron diffraction pattern (SAEDP) of the Ag-Co/C 1:3 (atomic ratio) supported on Vulcan carbon XC-72 catalyst, deposited on an amorphous carbon film.

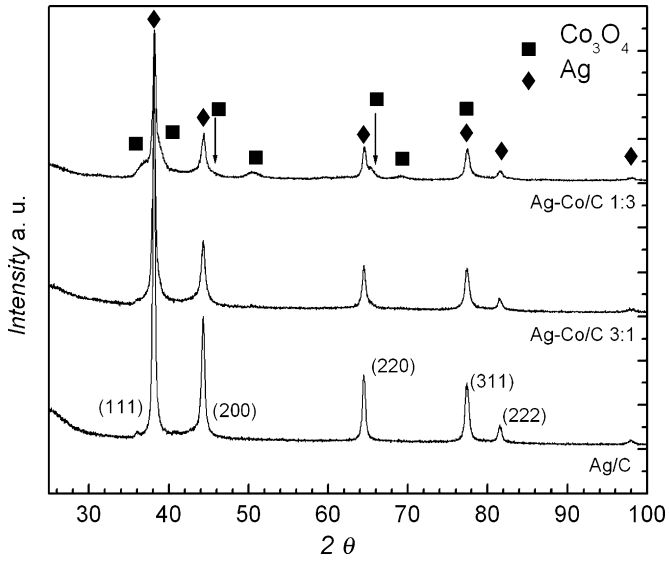

Fig. 4. X-ray diffraction (XRD) patterns for the Ag/C, Ag-Co/C 3:1 and 1:3 catalysts.

the reduction of Ag_2O back to metallic silver. The comparison between the CV curves shows a shift to the cathodic direction of the silver oxide reduction peak position with the increasing of the Co content in the Ag-Co/C catalysts. This phenomenon shows a stronger interaction between adsorbed oxygenated species on the Ag-Co compared to that on pure Ag. The presence of cobalt in the catalysts is evident only for Ag-Co/C 1:3 and Co/C by an oxidation peak located around 0.1 V versus Hg/HgO.

Steady state polarization curves for the ORR and the currents for the HO_2^- oxidation in the ring obtained at several rotation rates for the Ag/C catalyst are shown in Fig. 6. The expected increase of the limiting diffusion current density in the disk (Fig. 6b) is observed as a function of the rotation rate. On the other hand, the ring response (Fig. 6a) clearly denotes formation of HO_2^- as an intermediate of the ORR [31]. Fig. 7 compares

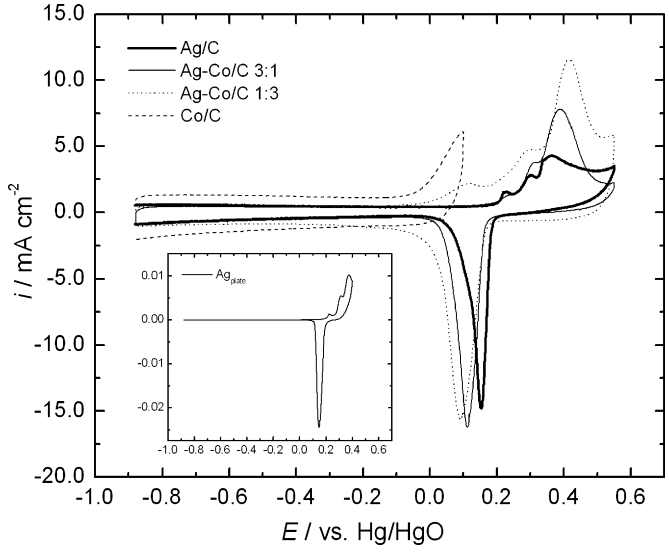

Fig. 5. Cyclic voltammograms for the Ag/C, Ag-Co/C and Co/C catalysts in N_2 saturated 1.0 mol L^{-1} KOH electrolyte at 0.1 V s^{-1}.

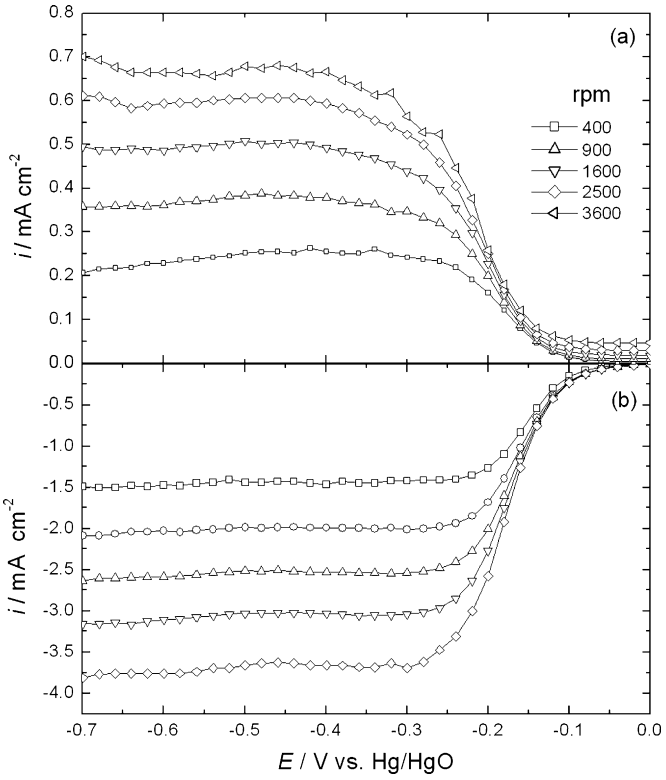

Fig. 6. Steady state polarization curves at different rotation rates for the ORR on Ag/C catalyst electrode in O_2 saturated 1.0 mol L^{-1} KOH electrolyte. (a) Ring current density (per geometric area) and (b) disk current density (per geometric area).

the ring/disk results at 1600 rpm for the different electrocatalysts. The result for a Pt/C catalyst is included for comparison. It is noted that the ORR limiting current densities for the Ag-based catalysts are higher than that for Vulcan carbon, and lower than that for Pt/C. Also, the bimetallic catalysts present slight higher limiting current densities in relation to Ag/C.

The disk polarization data at several rotation rates for each catalyst were used to construct Levich curves, as shown in Fig. 8. It is seen that the Levich plots are straight lines with different slopes, confirming that the number of electrons (n) involved in the ORR is dependent of the electrocatalyst material but independent on the rotation rate [32]. Fig. 8 also shows that the intercepts ($w^{1/2} \rightarrow 0$) of the Levich lines are not exactly zero as predicted by Eq. (1), but rather they assume values close to 0.2–0.4 mA cm^{-2}. These must correspond to current contributions not included for the derivation of Eq. (1), or represent a deviation of the behavior not predicted by this equation. Values of n were calculated from the slope of the Levich lines for all catalysts using Eq. (1):

$$i_d = 0.620nFAD_0^{2/3}\varpi^{1/2}\upsilon^{-1/6}C_0^* \quad (1)$$

where i_d is the limiting diffusion current density, F the Faraday constant, D_0 the oxygen diffusion coefficient, ϖ the rotation rate in rpm, υ the kinematic viscosity of the solution, and C_0^* is the oxygen solubility in the electrolyte. These calculations were made taking the Levich plot for the 60% Pt/C catalyst in the same medium as reference, and assuming $n = 4$ in this case

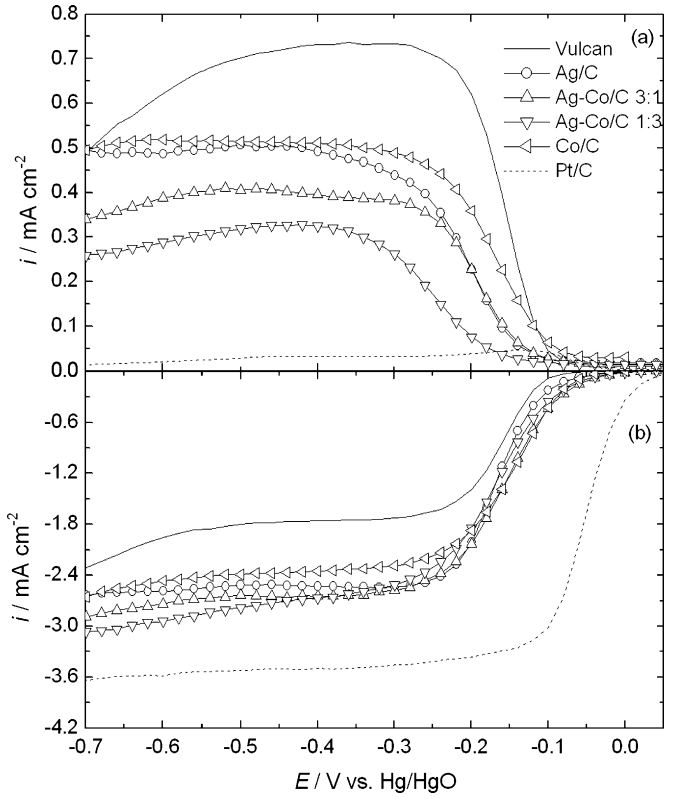

Fig. 7. Steady state polarization curves for the ORR on the Vulcan carbon powder, Co/C, Ag/C, Ag-Co/C and Pt/C catalysts in KOH 1.0 mol L^{-1} at 25 °C. (a) Ring current density (per geometric area) and (b) disk current density (per geometric area). $\omega = 1600$ rpm.

[32]. In all cases in Fig. 8 at higher electrode rotation rates, as the diffusion is fast, the rate-determining step may suffer from the influence of the kinetic control. So, the last points for all electrodes may not follow the Levich equation. Thus, if one takes the lower rotation rates, a slight increase of the Levich slope for Ag-Co/C compared to Ag/C can be noted. Although very small,

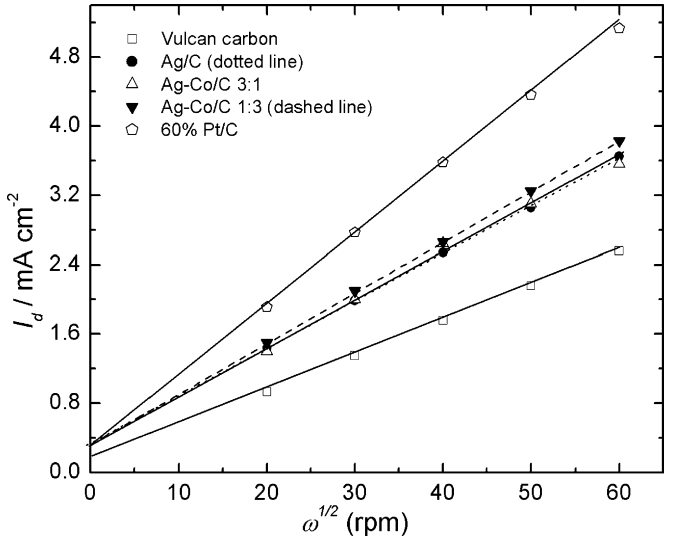

Fig. 8. Levich plots for the ORR on the Ag/C and Ag-Co/C catalysts compared to that obtained on Vulcan carbon and 60% Pt/C in KOH 1.0 mol L^{-1}.

an increase can be noted in the slope of the Levich curves for the Ag-Co/C compared to Ag/C. The calculated number of electrons resulted 2.7 for Ag/C, and 2.9 and 3.0 for Ag-Co/C 3:1 and 1:3 materials. The slight increase in the number of electrons for Ag-Co/C is also evidenced in the polarization curves presented in Fig. 7, which show an increase in the limiting density current for Ag-Co/C and, consequently, decreasing ring current signal. In the Co/C and Ag-Co/C catalysts, it is evident that the Co atoms are mainly in the form of Co_3O_4 and, into a lower extent, in the form of Co_2O_3. Many authors [33–36] have demonstrated that oxides and mixed oxides of transition metals are reasonable electrocatalysts for the ORR. In Co spinel oxides, like Co_3O_4, the O_2 reduction in alkaline media proceeds mainly through the 4-electrons pathway, while in lower valence oxides (NiO, CoO or their solid solutions, Co_2O_3) the reaction proceeds through the 2×2-electons pathway, with formation of HO_2^- as intermediate [36]. In the present work, the polarization curve for the Co/C material presented in Fig. 7 does not show a total 4-electrons pathway, as evidenced by the lower limiting current compared to that for the Pt/C catalyst. As further discussed below, this is probably due to the participation of the carbon particles and of the Co_2O_3 phase present on the Co-oxide segregated phases, as evident from the XRD results, in the overall oxygen reduction process.

Previous works have shown that on alkaline solutions, the ORR occurs mainly through the 4-electron mechanism in bulk Ag, and the 2-electron process in the Vulcan carbon [32,37]. In the present work, Fig. 7 shows that the onset potentials for the ORR on silver and on silver-cobalt bimetallic particles are close to that for Co/C and the Vulcan carbon. So, it is highly possible that for the Ag/C and Ag-Co/C particles the reaction occurs in parallel on Co_3O_4 and Ag sites, following the 4-electrons pathway, and on carbon and on the Co_2O_3 phase, following the 2-electrons pathway:

$$O_2 + 2e^- + H_2O \rightarrow HO_2^- + OH^- \quad (\text{carbon}, Co_2O_3) \qquad (2)$$

$$O_2 + 4e^- + 2H_2O \rightarrow 4OH^- \quad (Ag, Co_3O_4) \qquad (3)$$

The size of the Ag-based catalyst particles are relatively larger compared to that for Pt/C (3.0 nm). This reduces the surface area, resulting in a high contribution of the carbon support on the 2-electrons pathway of the ORR electrocatalysis. As a balance, the number of electrons close to 3.0 obtained from the Levich plots for all Ag-based catalysts indicates that only ca. 50% of the total process is catalyzed by the Ag and/or Co_3O_4 sites. However, another fact which may influence the number of electrons involved in the ORR is the presence of impurities in the electrolyte. For Ag, it was shown [37] that the 4-electron pathway is switched to the 2-electron route due to the presence of impurities in the electrolyte, because they difficult the bridge-adsorption of O_2 on the catalyst sites. In the present work no evidence of such an effect was found.

The electrocatalytic activity for the ORR in the different ultra thin layer electrodes can be more adequately compared in terms of mass-transport corrected Tafel plots [32]. These results are presented in Fig. 9 for plots built with the currents normalized by the mass of metal (Fig. 9a), mass of Ag (Fig. 9b) and by the

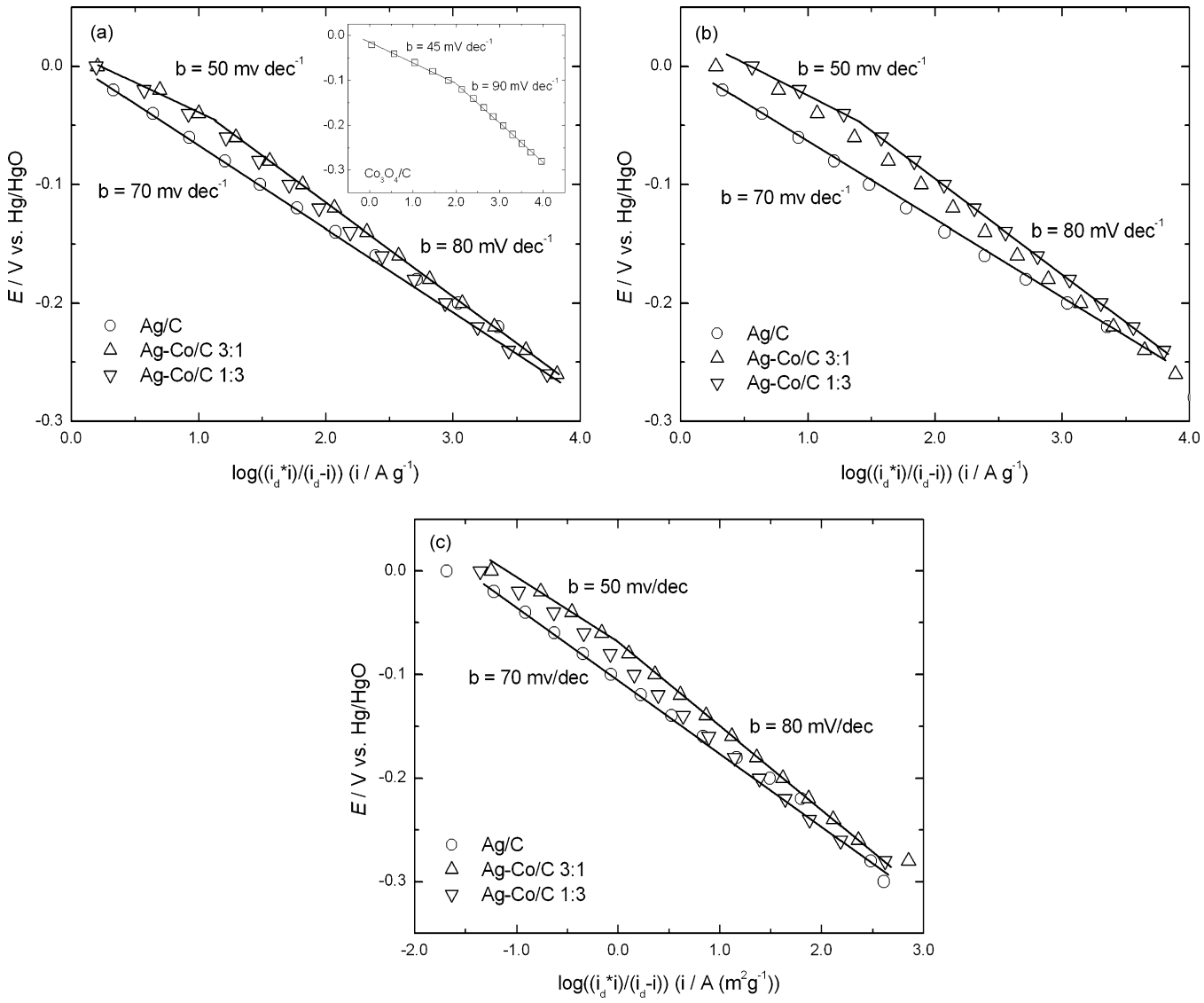

Fig. 9. Mass-transport corrected Tafel plots for the ORR on Ag/C and Ag-Co/C catalysts with, (a) currents normalized per mass of metal in the catalyst layer. Inset: result obtained for Co/C. (b) Currents normalized per mass of Ag in the catalyst layer. (c) Currents normalized per metal surface area in O_2 saturated 1.0 mol L^{-1} KOH electrolyte. $\omega = 1600$ rpm.

surface area of the catalyst layer (Fig. 9c) as determined from the crystallite sizes obtained by XRD [38]. For the Co/C and Ag-Co/C catalysts, two different Tafel linear regions are observed, with slopes close to 45–90 and 50–90 mV dec^{-1} for low and high overpotentials, respectively. The presence of two Tafel slopes would be explained in terms of the coverage of adsorbed oxygen, as in the case of platinum, which can be described by the Temkin isotherm (high coverage) at low overpotentials and the Langmuir isotherm (low coverage) at high overpotentials [39]. For the Ag/C catalyst, only one linear region is clearly noted in Fig. 9 with a slope close to 70 mV dec^{-1}. This would show that the ORR occurs following only one isotherm. It must be mentioned that, in all cases, as the onset potentials of the ORR on the Ag-based catalysts are close to that for Vulcan carbon or Co/C, the Tafel diagrams can be interpreted in terms of a combined participation of the carbon, cobalt oxides and silver in the catalysis of the ORR.

Fig. 9a–c evidence higher catalytic activities for the Ag-Co/C materials compared to Ag/C, even for the currents normalized by the crystallite surface area (Fig. 9c), but the effect is little pronounced. Since the Ag-Co/C bimetallic particles are formed by segregated phases, and very low quantity of Co atoms are inserted in the Ag metal lattice structure, the increase in the O_2 reduction kinetic cannot be assigned to changes in the Ag lattice. A hypothesis for explaining the enhanced ORR electrocatalysis in acid media on the Ag-Co/C compared to Ag/C material was discussed by Bard and co-workers [22]. This hypothesis assumes a simple mechanism in which one of the metals (Co) is responsible for breaking the O–O bond; then the adsorbed atomic oxygen atoms migrate to the other metal (Ag), where the electroreduction step takes place. However, an important result for clarifying this discussion is observed in the cyclic voltammograms in Fig. 5, where it is noted that the silver oxide reduction peak is shifted to lower potentials for

Ag-Co/C catalysts, compared to Ag/C, indicating a stronger adsorbed-oxygen interaction with the Ag surface sites. These results suggest that an increased activity of the Ag atoms in the Ag-Co/C materials for the ORR is due to the higher interaction of adsorbed oxygen with Ag. This facilitates the O–O bond splitting, increasing the ORR kinetics compared to Ag/C.

4. Conclusions

Silver-cobalt bimetallic particles dispersed on a carbon powder were investigated as electrocatalysts for the ORR in alkaline media; this is in contrast to previous work where acid electrolyte was employed. TEM measurements showed a heterogeneous crystallite size distribution and indicated a segregation phase of cobalt mainly as Co_3O_4 for the bimetallic Ag-Co/C catalysts. The characterization of the materials by XRD clearly suggest a negligible decrease in the Ag fcc lattice parameter, which was ascribed to a negligible Co insertion into the Ag structure; the presence of a Co_3O_4 segregated phase in the Ag-Co/C bimetallic particles was also evident.

Cyclic voltammetry results showed a shift to the cathodic direction of the silver oxide reduction peak positions for the Ag-Co/C catalysts, compared to Ag/C. This was associated with higher interaction of the adsorbed oxygen species with Ag on the Ag-Co/C materials, compared to that on Ag/C. Levich plots obtained from rotating disk electrode data for Ag/C and Ag-Co/C have shown that the number of electrons involved in the ORR slightly increased with increasing Co content. This was associated with a parallel route for the reaction pathways: on Ag and on the Co_3O_4 sites, following the 4-electron pathway, and on carbon and on Co_2O_3 sites, following the 2-electron pathway. The analysis of the polarization results suggested higher activity for the ORR on Ag-Co/C materials compared to Ag/C, but the effect is hardly pronounced. This was ascribed to a stronger interaction of oxygen with the Ag atoms, which facilitated the O–O bond splitting, increasing the ORR kinetics.

Acknowledgments

The authors thank the Fundação de Amparo à Pesquisa do Estado de São Paulo (FAPESP), the Conselho Nacional de Desenvolvimento Científico e Tecnológico (CNPq), and Coordenação de Aperfeiçoamento de Pessoal de Nível Superior (CAPES), Brazil, for financial assistance.

References

[1] J. Zhang, Y. Mo, M.B. Vukimirovic, R. Klie, K. Sasaki, R.R. Adzic, J. Phys. Chem. B 108 (2004) 10955.
[2] U.A. Paulus, A. Wokaun, G.G. Sherer, T.J. Shmidt, V. Stamenkovic, V. Radmilovic, N.M. Markovich, P.N. Ross, J. Phys. Chem. B 106 (2002) 4181.
[3] F.H.B. Lima, E.A. Ticianelli, Electrochim. Acta 49 (2004) 4091.
[4] F.H.B. Lima, M.J. Giz, E.A. Ticianelli, J. Braz. Chem. Soc. 16 (2005) 328.
[5] L. Xiong, A.M. Kannan, A. Manthiram, Electrochem. Commun. 4 (2002) 898.
[6] S. Mukerjee, S. Srinivasan, M.P. Soriaga, J. McBreen, J. Phys. Chem. 99 (1995) 4577.
[7] M. Min, J. Cho, K. Cho, H. Kim, Electrochim. Acta 45 (2000) 4211.
[8] T. Toda, H. Igarashi, M. Watanabe, J. Electroanal. Chem. 460 (1999) 258.
[9] A.S. Arico, A.K. Shukla, H. Kim, S. Park, M. Min, V. Antonucci, Appl. Surf. Sci. 172 (2001) 33.
[10] J. Zhang, M.B. Vukmirovic, Y. Xu, M. Mavrikakis, R.R. Adzic, Angewandte 44 (14) (2005) 2132.
[11] B. Hammer, J.K. Nørskov, Surf. Sci. 343 (1995) 211.
[12] J.R. Kitchin, J.K. Nørskov, M.A. Barteau, G. Chen, J. Chem. Phys. 120 (2004) 10240.
[13] B. Hammer, J.K. Nørskov, Adv. Catal. 45 (2000) 71.
[14] J. Greeley, J.K. Nørskov, M. Mavrikakis, Annu. Rev. Phys. Chem. 53 (2002) 319.
[15] L. Mao, D. Zhang, T. Sotomura, K. Nakatsu, N. Koshiba, T. Ohaka, Electrochim. Acta 48 (2003) 1015.
[16] Y.L. Cao, H.X. Yang, X.P. Ai, L.F. Xiao, J. Electroanal. Chem. 557 (2003) 127.
[17] M.L. Calegaro, F.H.B. Lima, E.A. Ticianelli, J. Power Sources 158 (2006) 735.
[18] M. Chatenet, L. Genies, M. Aurousseau, R. Durand, F. Andolfatto, J. Appl. Electrochem. 32 (2002) 1131.
[19] M. Chatenet, M. Aurousseau, R. Durand, F. Andolfatto, J. Electrochem. Soc. 150 (2003) 47.
[20] L. Demarconnay, C. Coutanceau, J.-M. Leger, Electrochim. Acta 49 (2004) 4513.
[21] F.H.B. Lima, C.D. Sanches, E.A. Ticianelli, J. Electrochem. Soc. 152 (7) (2005) A1466.
[22] J.L. Fernandez, D.A. Walsh, A.J. Bard, J. Am. Chem. Soc. 357 (2005) 357.
[23] A.R. West, Solid State Chemistry and its Applications, Wiley, New York, 1984.
[24] T.J. Schmidt, H.A. Gasteiger, G.D. Stäb, P.M. Urban, D.M. Kolb, R.J. Behm, J. Electrochem. Soc. 145 (1998) 2354.
[25] JCPDS—Joint Committee on Powder Difraction Standards, Pennsylvania, 1980.
[26] G. Orozco, M.C. Perez, A. Rincon, C. Gutierrez, J. Phys. Chem. 100 (1996) 8389.
[27] G. Orozco, M.C. Perez, A. Rincon, C. Gutierrez, J. Electroanal. Chem. 495 (2000) 71.
[28] E.R. Savinova, P. Kraft, B. Pettinger, K. Doblhofer, J. Electroanal. Chem. 430 (1997) 47.
[29] S. Chen, B. Wu, C. Cha, J. Electroanal. Chem. 420 (1997) 111.
[30] T. Itoh, T. Maeda, C. Horie, Surf. Sci. 389 (1997) 212.
[31] R.R. Adzic, in: J. Lipkowski, P.N. Ross (Eds.), Electrocatalysis, vol. 5, VCH, New York, 1998, p. 197.
[32] J. Perez, E.R. Gonzalez, E.A. Ticianelli, Electrochim. Acta 44 (1998) 1329.
[33] S. Trasatti, in: J. Lipkowski, Ph. Ross (Eds.), Elecrochemistry of Novel Materials, vol. III, VCH I&, New York, 1994, p. 207.
[34] M.R. Tarasevich, A. Sadkowski, E. Yeaaer, in: B.E. Conway (Ed.), Comprehensive Treaty of Electrochemistry, vol. 7, Plenum, New York, 1983, p. 301.
[35] N. Heller-Ling, M. Prestat, J.-L. Gautier, J.-F. Koenig, G. Poillerat, P. Chartier, Electrochim. Acta 42 (1997) 197.
[36] D. Yoke, A. Riga, R. Greeff, E. Yeager, Electrochim. Acta 13 (1968) 1351.
[37] P. Fischer, J. Heitbaum, J. Electroanal. Chem. 112 (1980) 231.
[38] E. Antolini, R.R. Passos, E.A. Ticianelli, Electrochim. Acta 48 (2002) 263.
[39] A. Damjanovic, M.A. Genshaw, J.O'M. Bockris, J. Phys. Chem. 45 (1964) 4057.